The self-organizing properties of squid reflectin protein

RYAN M. KRAMER, WENDY J. CROOKES-GOODSON AND RAJESH R. NAIK*

Air Force Research Laboratory, Materials and Manufacturing Directorate, Biotechnology Group, Wright-Patterson Air Force Base, Dayton, Ohio 45433, USA
*e-mail: rajesh.naik@wpafb.af.mil

Published online: 3 June 2007; doi:10.1038/nmat1930

Reflectins, a recently identified protein family that is enriched in aromatic and sulphur-containing amino acids, are used by certain cephalopods to manage and manipulate incident light in their environment. These proteins are the predominant constituent of nanoscaled photonic structures that function in static and adaptive colouration, extending visual performance and intra-species communication. Our investigation into recombinantly expressed reflectin has revealed unanticipated self-assembling and behavioural properties, and we demonstrate that reflectin can be easily processed into thin films, photonic grating structures and fibres. Our findings represent a key step in our understanding of the property–function relationships of this unique family of reflective proteins.

Aquatic and terrestrial organisms have evolved complex optical structures that modulate light using micro- and nanostructures[1–3]. Organisms that live in aquatic environments where sunlight readily penetrates are able to manage incident light to produce body patterning that gives them a selective advantage[4–6]. Cephalopods, in particular, can manipulate their overall body colouration using a combination of transparency, controllable pigmentation, preferential scattering of light and photonic structures that guide and reflect light[5]. These photonic structures are often found in the form of diffraction gratings or multilayer stacks in reflective tissues and are visually associated with spectral iridescence. The reflectivity of the latter results from alternating layers of high- and low-refractive-index dielectrics, creating thin-film interference[2].

The reflective platelets from the Hawaiian bobtail squid, *Euprymna scolopes* (Cephalopoda: Sepiolidae), were found to be composed of proteins, termed reflectins, that exhibit a skewed and unique amino-acid composition and five repeating domains[7]. The reflectin protein characterized herein, reflectin 1a, originates from a specialized tissue of imperfectly packed multilayer stacks termed the light-organ reflector (see Supplementary Information, Fig. S1a,b)[7–10]. This multilobed reflector directs light produced by bacterial symbionts ventrally into the surrounding seawater, mimicking downwelling moon- and starlight and preventing predators from tracking the squid from below[11,12]. Proteins found in the reflective structures of other cephalopod species have recently been shown to share homology with the reflectin family of proteins from the bobtail squid, suggesting that reflectin proteins may represent a ubiquitous, yet novel, optical nanostructural material among cephalopods[13] (M. Izumi *et al.*, personal communication).

Reflectins are compositionally different from the subset of reflective elements found in other organisms, which are mostly composed of the purine crystals guanine and hypoxanthine[9]. The evolutionary selection of a protein-based reflective material in cephalopods may contribute to an increased complexity of the photonic structure. For instance, protein modification and aggregative state have been shown to be critical for the dynamic iridescence identified in several squid species[14,15]. This dynamic reflection has been hypothesized to occur by altering platelet and inter-platelet thicknesses in the multilayer reflector and/or altering the overall effective refractive index of the intra-platelet material. This allows the entire visible spectrum to be reflected from a single platelet stack[15]. On the basis of the findings that reflectance from mantle iridophores of *Lolliguncula brevis* can be shifted from long wave (red) to short wave (blue) through the exogenous addition of acetylcholine and calcium ionophores, the reflectin proteins represent a structurally adaptive biopolymer that could be explored by the material science community[14–16].

In this paper, we explore for the first time the biophysical properties associated with this protein-based reflective material. Our study initially highlights *in vitro* self-assembling properties of recombinant reflectin through an investigation into a number of different protein-refolding conditions. We then further demonstrate techniques for reflectin thin-film production and monitor the structural colouration produced from these films as a function of vapour-induced film swelling. The combination of the self-assembling property of reflectin and an ionic liquid solvent can lead to the directed formation of surface diffraction gratings. We conclude our studies by showing that the native reflectin material can be easily formed into fibres.

For many structural proteins, it has been shown that protein self-assembly into ordered arrays is critical for function[17,18]. For example, amelogenin, a structural protein associated with dental enamel, forms microribbons resulting from the aggregation of an insoluble protein precursor into nanospheres that multimerize to form a highly ordered structure[19]. Owing to the fact that ordered arrays are the hallmark of multilayer reflectors (Fig. 1a), we speculated that reflectin, which is composed of repeating protein domains and insoluble in most organic and inorganic solvents[8], might follow a similar assembly mechanism. We first expressed and purified reflectin 1a from *Escherichia coli* to obtain recombinant reflectin for further investigation (see the Methods section and Supplementary Information, Fig. S1c,d). Purified recombinant reflectin was diluted with deionized water to reduce the overall buffer concentration to >3 M guanidine hydrochloride for subsequent refolding trials. Further dilution of the reflectin protein led to the spontaneous formation of protein nanospheres

©2007 Nature Publishing Group

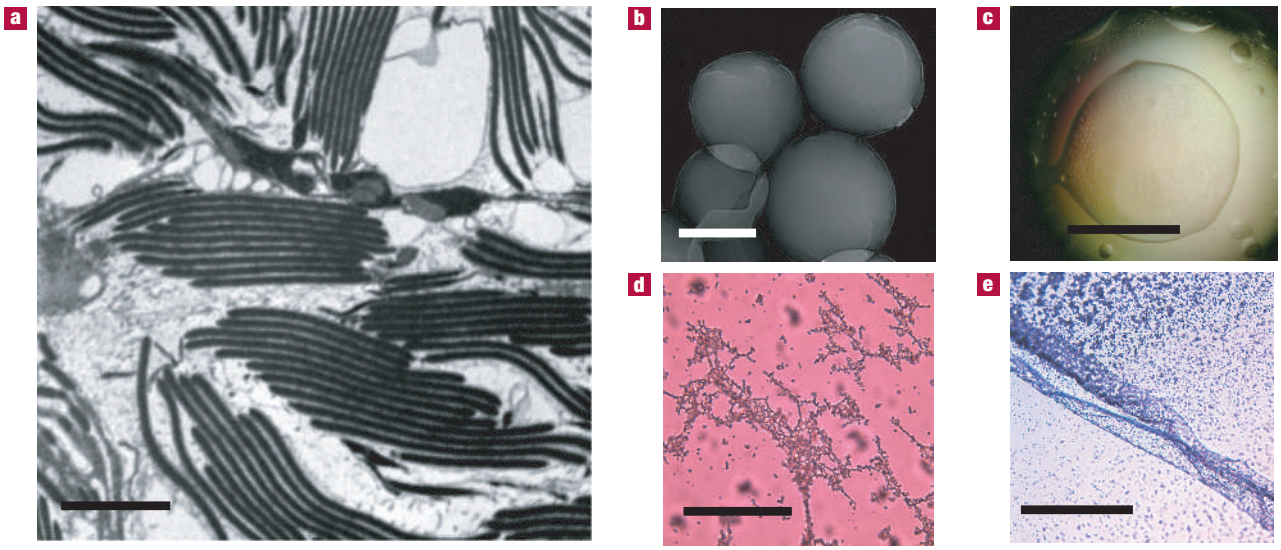

Figure 1 Light-organ platelets and native self-assembly of reflectin 1a protein from an insoluble precursor. a, Cross-sectional TEM micrograph of reflectin platelet stacks from the light organ of *Euprymna scolopes*. Scale bar: 5 μm. **b**, TEM micrograph of spherical reflectin particles following dialysis from 7 M guanidine hydrochloride into water. Scale bar: 50 nm. **c**, Optical micrograph of a microdialysis button containing reflectin dialysed into water from a starting solution containing 55 mM Tris pH 8.2, 264 mM NaCl, 11 mM KCl, 0.055% polyethylene glycol and 7 M guanidine hydrochloride forming a bulk aggregate. Scale bar: 1 mm. **d**, Optical micrograph of a similar microdialysis button with the same conditions as in **c** but with the inclusion of 100 mM reduced glutathione and 10 mM oxidized glutathione. Scale bar: 20 μm. **e**, Mature ribbon-like structure formed from the aggregation of filamentous structures. Scale bar: 100 μm.

with dimensions spanning 50–1,000 nm (Fig. 1b). To understand if improper folding of the protein led to the formation of the protein nanospheres and to explore whether the protein could be refolded into a more water-soluble form, we used a screening method to analyse the effects of pH, polar additives, detergents, ionic strength, osmolytes and redox environment on the recombinant protein. Micro-dialysis of reflectin 1a into various buffers resulted in two general types of aggregative structures. Optically clear bulk precipitation was seen in non-reducing conditions (Fig. 1c) and filamentous protein structures were observed in reducing conditions (Fig. 1d), controlled through the addition of a 10:1 ratio of reduced to oxidized glutathione. After several weeks at 4 °C, the filamentous structures formed a webbed structure that resulted in the supramolecular assembly of thin ribbons (Fig. 1e). The filamentous structures of reflectin are not amyloid-type fibrils as they differ greatly in overall morphology and X-ray structure[20]. Supramolecular assembly has been theorized to occur through intermediately sized structures, and both dimers and trimers of the purified reflectin protein are clearly seen in SDS–polyacrylamide gel electrophoresis gels even under highly denaturing conditions (see Supplementary Information, Fig. S1d). The reflectin polypeptide has five highly conserved repeat regions with some of these repeat regions ending in a conserved cysteine residue[8]. Therefore, the influence of the redox environment may not only effect the *in vitro* assembly of the reflectin but may have a more general role in determining the tertiary and quaternary structure of the protein *in vivo*.

We next sought to determine if recombinant reflectin can be processed into films and fibres for further characterization. Films of the precipitated reflectin protein dissolved in 1,1,1,3,3,3 hexafluoroisopropanol (HFIP) were cast using a flow-coating technique (Fig. 2a). By varying the protein concentration, we were able to cast films of different thicknesses with the general correlation that more dilute solutions gave rise to films with decreased thickness. On the basis of the overall thickness of the cast films, different structural colours arose from the films owing to thin-film interference (Fig. 2b). We were able to cast films with uniform thickness that covered the entire visible spectral range. In addition to the production of films with uniform thickness, gradient films were cast onto silicon wafers by adjusting the blade tilt on the flow-coating apparatus (Fig. 2c). Spectral data in the visible region were gathered from several spots on the gradient film and representative spectra across the entire visible region (400–750 nm) were observed (Fig. 2d).

Using these flow-coated films, we were also able to determine the refractive index of recombinant reflectin. *In vivo*, the photonic structures reflect light through alternating layers of high and low-index materials, with the high-index layer comprising reflectins. The refractive index of recombinant reflectin was calculated to be 1.591 ± 0.002 (see Supplementary Information, Fig. S2). To our knowledge, this is the highest reported refractive index for a naturally occurring protein. The elevated refractive index of reflectins compared with other proteins can most likely be attributed to the unique amino-acid composition of the protein, which is composed of 43.8% aromatic and sulphur-containing amino acids.

Mäthger *et al.* and Hanlon and co-workers have shown that an iridescent iridophore within the squid mantle can reflect multiple colours[15,16]. Recent findings by Morse *et al.* have also shown that post-translational modification of reflectin may dictate how these proteins change their aggregative state and the overall reflectance of the iridophores (M. Izumi *et al.*, personal communication). For photonic applications, post-translational modifications would be difficult to reproduce in devices and other methods to replicate dynamic reflectance would be desirable. For example, we can imagine introducing reversible optical transitions into thin films using swelling effects. When exposed to water, methanol and ethanol vapours, reflectin films exhibit a dramatic spectral reflectance shift common to polymer-based thin films (Fig. 3a). Because thin-film interference coatings give rise to multiple

©2007 Nature Publishing Group

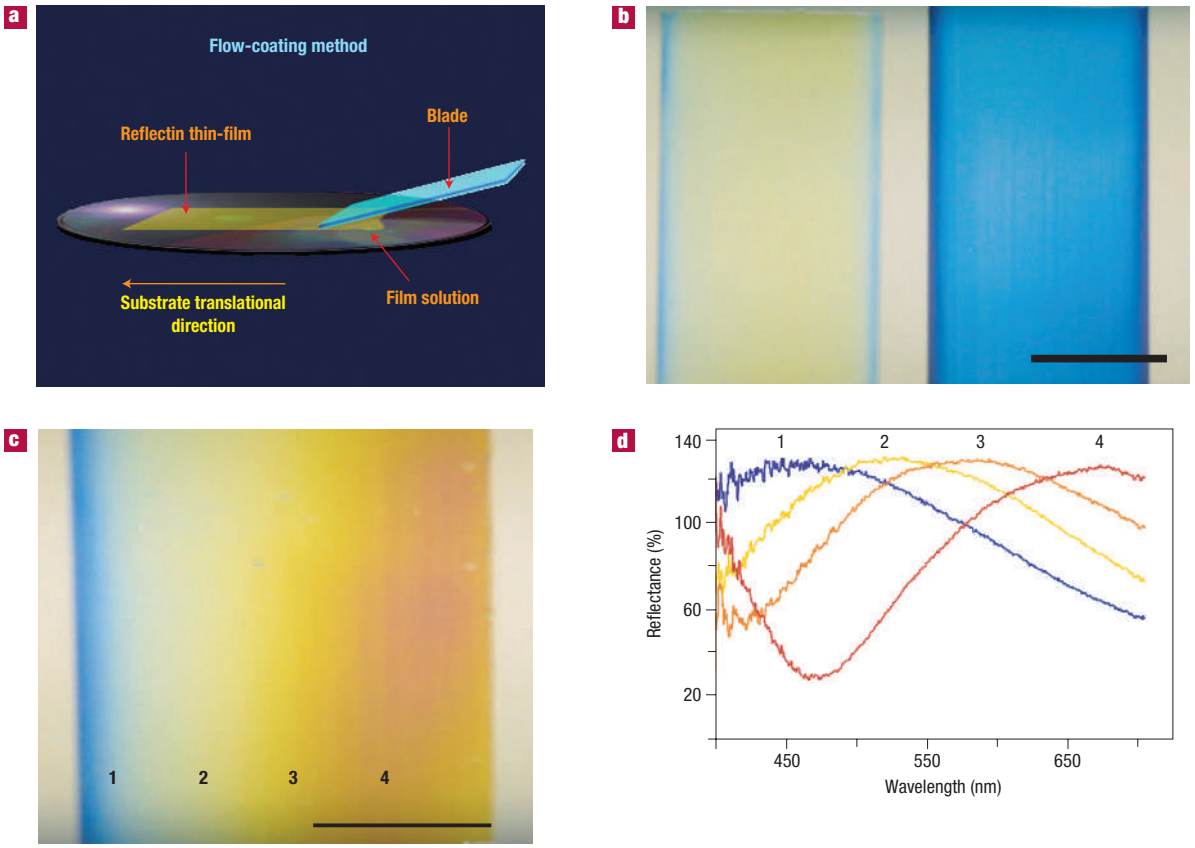

Figure 2 Solution casting of recombinant reflectin thin films. a, Schematic diagram of the flow-coating technique for casting thin films of reflectin protein onto a silicon-wafer substrate. **b**, Reflectin films exhibiting uniform thicknesses cast from a 15% w/w (left) and 10% w/w (right) reflectin/HFIP solution. Scale bar: 2 cm. **c**, Gradient reflectin film cast by adjusting the blade tilt during its translation over the substrate. Scale bar: 1.5 cm. **d**, Spectral analysis of several points along the gradient film in **c** showing constructive and destructive interference resulting from thin-film interference. Reflectance from regions outside the protein film showed a flat baseline at 100% that spanned the entire visible spectrum (data not shown).

constructive and destructive interference fringes, we determined whether the observed colour shift in the films was due to a blue- or red-shift of the interference spectrum. Time-lapse spectral analysis, which monitored the visible spectrum between 400 and 800 nm, showed that following the administration of water vapour to the reflectin film, the primary peak centred around 760 nm shifted towards longer wavelengths out of the recorded spectrum. Simultaneously, a secondary peak centred around 400 nm appeared, giving rise to a blue reflectance from the film (Fig. 3b). As long as the water vapour was administered to the film, this constructive fringe continued to shift towards longer wavelengths. When the vapour stimulus was removed, the constructively interfering peak blue-shifted out of the detected range as the original fringe shifted from the infrared wavelengths back into the detectable range, restoring the original red reflectance. White-light interferometry of thin films exposed to water vapour revealed that on exposure to vapour a dramatic increase in film thickness occurred. The film thickness increased from ~120 nm to 207 nm in the presence of water vapour (Fig. 3c). During film swelling, the increase in film thickness resulted in detectable red-shift of the visible spectra and dominated any effect of decreasing refractive index owing to water sorption, which would have caused a blue-shift in the spectrum.

A second method also generated thin films of reflectin with interesting properties. Ionic liquids have garnered much attention owing to their ability to aid in dissolution and processing of insoluble proteins such as silk and cellulose[21,22]. Precipitated reflectin was found to be soluble in the ionic liquid, 1-butyl-3-methylimidazolium chloride (BMIM). Thin films cast from reflectin dissolved in BMIM were immersed in a water bath at a constant rate to extract the BMIM from the film (Fig. 4a). The protein immediately phase separated on the substrate as the ionic liquid actively diffused from the cast film and spontaneously formed a surface diffraction grating exhibiting iridescence under polychromatic light (Fig. 4b–d). The grating structure, observable with optical microscopy and scanning electron microscopy (SEM), consistently assembled parallel to the dipping direction (Fig. 4b–d). Iridescence was observed even while the films were still submerged in the deionized water, indicating that the gratings did not result from drying effects but rather from their insertion into the water bath. We were able to control grating spacing by varying the dipping velocity of the substrate with resultant spacings spanning 1.8−18 μm. The topographical height of the grating remained consistent throughout each sample as determined by white-light interferometry. For example, the topographic height of a surface grating with 2 μm spacing was determined to be 293 ± 35 nm over 1 mm^2 (Fig. 4e). Overall, we determined that increased dipping velocity resulted in decreased grating spacing as summarized for three velocities in Fig. 4f.

Reflectin gratings showed remarkably even spacing and extended defect free for several millimetres. The compressed composite SEM image in Fig. 4g shows a 100 μm × 2 mm area of the

©2007 Nature Publishing Group

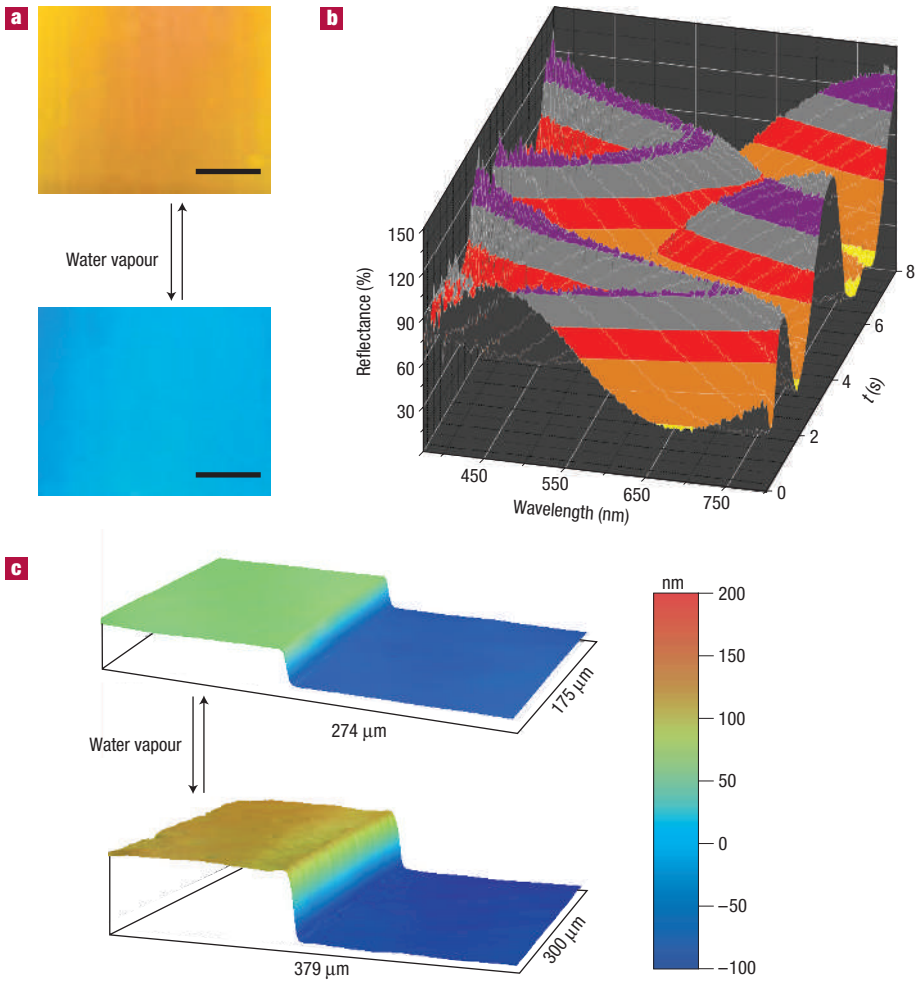

Figure 3 Reflectin films exhibit shifts in the spectral interference peaks due to film swelling. a, Reflectin thin-film exhibiting reddish reflectance (upper frame) reversibly exhibited a blue reflectance following exposure to water vapour (lower frame). Scale bar: 0.5 cm. **b**, Time-lapse spectral analysis of a reflectin thin film on exposure to water vapour. A red reflective thin film was exposed to water vapour and immediately turned blue (time, $t = 0$ s) with a maxima at 430 nm. Continued exposure to water vapour resulted in a red-shift of the peak until the vapour source was removed ($t = 1$ s). The peak interference fringe shifted towards shorter wavelengths, and returned to its original reflectance at $t = 5$ s. The cycle was repeated and water vapour administered from $t = 5$ s to $t = 7$ s. **c**, White-light interferometry of a reflectin thin film before (upper frame, thickness = 120 nm) and during (lower frame, thickness = 207 nm) administration of water vapour exhibiting dramatic film swelling on exposure to water vapour.

grating. As spacing increased within the gratings, we also observed a greater number of defects such as dislocations, although regular spacing at localized dislocations was often restored within 30 μm from each site (see Supplementary Information, Fig. S3a). High-resolution SEM images of the gratings revealed that each ridge within the grating was composed of small entangled fibrils (see Supplementary Information, Fig. S3b) that were similar to fibrils formed in a separate experiment when the reflectin/BMIM solution was spotted onto an air–water interface (see Supplementary Information, Fig. S3c,d). The induced formation of optical grating structures using this technique resulted from a mass loss as the ionic liquid diffused away from the thin films, leaving behind phase-separated reflectin. Because grating structures always formed parallel to the dipping direction, we hypothesize that the entrance angle dictates the spatial orientation of the reflectin gratings. Increasing the ionic strength of the coagulation bath using sodium chloride resulted in the distortion and loss of the grating structure (see Supplementary Information, Fig. S4). These results indicate that local ionic interactions contribute to the assembly process. We are currently examining the effects of film thickness and protein concentration as other factors that spatially influence these microstructures.

Although we used exotic solvents for film preparations, reflectin could also be processed from a precipitate. Precipitation of reflectin resulted in a highly viscous material that could also be easily drawn into fibres with a smooth outer surface, optical clarity and diameters ranging from 500 nm to 150 μm (Fig. 5). Because secondary structural alignment in a sample is often increased during fibre pulling and extrusion, we carried out X-ray diffraction (XRD) on fibre bundles and single fibres to determine the possible structural alignment of the protein. Reflectin fibres consistently gave rise to a diffraction pattern with two general amorphous peaks centred at 1.0 nm and 0.44 nm (see Supplementary Information, Fig. S5). Methanol- and HFIP-soaked fibres, which have previously been shown to induce beta-sheet and alpha-helical secondary structures in other proteins[23,24], had no effect on the wide-angle

©2007 Nature Publishing Group

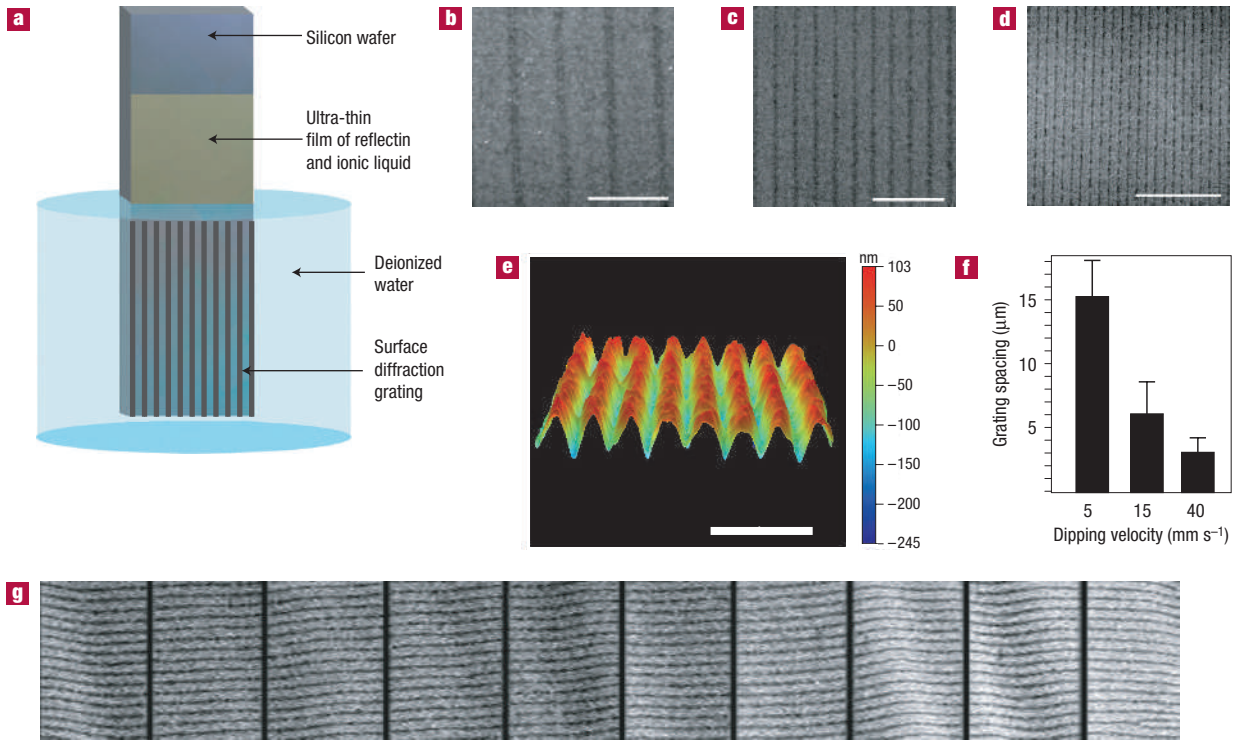

Figure 4 Surface diffraction gratings produced from reflectin/ionic liquid thin films. a, Schematic diagram of the technique used for the creation of reflectin-based surface diffraction gratings. **b–d**, Typical gratings formed using dipping velocities of 5 mm s^{-1} (**b**), 15 mm s^{-1} (**c**) and 40 mm s^{-1} (**d**). Scale bars: 20 μm. **e**, White-light interferometry of a surface grating produced with a 40 mm s^{-1} dipping velocity exhibiting uniform grating height and separation. Scale bar: 15 μm. **f**, Change in the diffraction grating spacing with respect to the dipping velocity. The error bars indicate standard deviation. **g**, Long-range order of reflectin-based surface gratings visualized through compressed composite SEM images of a 30 μm × 2 mm area. The vertical black lines denote where images were joined.

X-ray diffraction pattern and associated secondary structure. The absence of crystallinity in the processed reflectin fibres is ideal for many photonic applications because increased polycrystallinity in optical materials can cause anomalous scatter and optical loss. The recombinant reflectin fibres were also capable of condensing silica on their surfaces. Reflectin fibres when soaked in alkoxide precursor solution (tetramethyl orthosilicate), produced a silica coating on its external surface with the fibre acting as a condensation surface for the alkoxide precursor. SEM of a fractured fibre revealed a distinct core–cladding arrangement with silica nanoparticles formed on the fibre surface (see Supplementary Information, Fig. S6).

Ultimately, biomaterial research aims to explore naturally occurring materials for new paradigms in material design. Our investigation into the structure–property contribution from reflectin could shed light on how this protein might best be exploited. In this paper, we focused on the recombinant expression of reflectin and its processing, to understand its optical properties in relation to *in vivo* observations. In our characterization of the reflectin protein, we have also uncovered unique properties stemming from innate molecular properties contributed by the biopolymer. The ability of reflectin to organize into diffraction gratings that are defect free over long distances might lead to its use in bottom-up fabrication of photonic-crystal and bandgap devices[25,26]. In addition, the ability to fabricate reflectin-based films and fibres suggests that it can be exploited for use as an optoelectronic material. The self-assembled reflectin diffractions can also be used as scaffolds for the organization of inorganic nanomaterials. Finally, we note that our findings warrant detailed investigations into the relative contributions of the amino-acid sequence and structure of the reflectin polypeptide to fully understand the behaviour of this unusual family of proteins.

METHODS

MICROSCOPY

Optical microscopy was carried out with a Nikon Optical-Photo Polarizing Microscope and images were taken with a Nikon Digital Camera DYN1200. Electron micrographs were obtained using a Philips EM208 operating at 200 kV with a Noran Voyager energy-dispersive X-ray analysis system. SEM was carried out using an FEI XL FEG/SFEG/SIRION Environmental SEM.

RECOMBINANT REFLECTIN 1A EXPRESSION AND PURIFICATION

The reflectin 1a gene protein[7] (GenBank accession AY294649) coding region was optimized for *Escherichia coli* expression and synthetically produced and ligated into the pST50Tr-HISRef1a plasmid with an amino-terminal hexahistidine fusion tag. The pST50Tr-HISRef1a plasmid was then transformed into *Escherichia coli* BL21 (DE3) pLysS (Invitrogen). Expression was induced by the addition of 1 mM isopropyl-β-D-thiogalactoside (final concentration) when the cells reached an optical density at 600 nm of ~0.6. The cells were then grown for 5 h at 37 °C and harvested by centrifugation. Harvested cells were resuspended in 50 ml of buffer A (20 mM Tris-HCl, pH 8.0, 100 mM NaCl) and stored frozen. Thawed cells were ultrasonicated three times for 15 s in 15 ml batches at 40% power. The lysed crude cell suspension was centrifuged and inclusion body preparation carried out according to standard protocols. The final pelleted fractions from the inclusion body preparation were resuspended in 7 M guanidine hydrochloride and allowed to incubate overnight at 4 °C. Further purification of the His-reflectin 1a protein was carried out using metal-affinity low-pressure chromatography with 25 ml TALON Superflow resin using standard protocols.

©2007 Nature Publishing Group

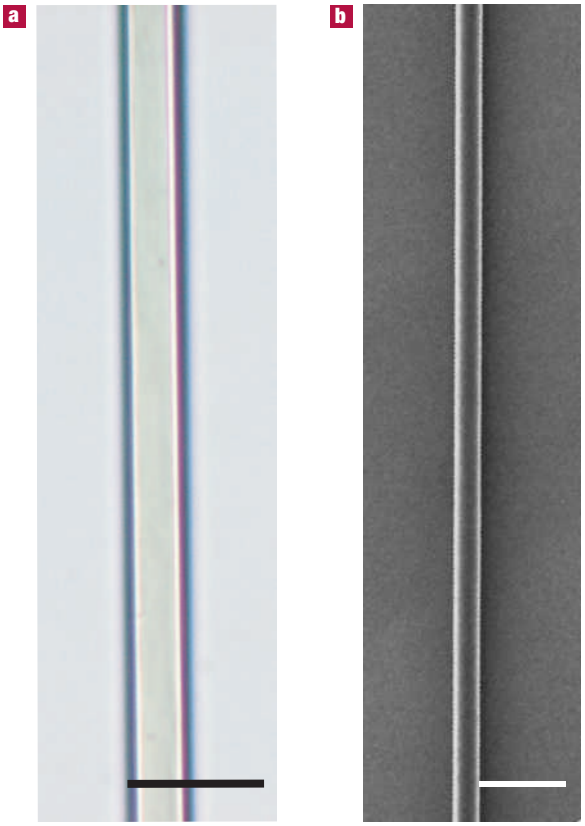

Figure 5 Reflectin 1a fibres pulled from bulk precipitated protein. a, Optical microscope image of reflectin fibre. Scale bar: 100 μm. **b**, Scanning electron micrograph of a smaller diameter fibre. Scale bar: 2 μm.

PROTEIN REFOLDING AND CRYSTALLIZATION TRIALS

TALON-purified reflectin was refolded by first dialysing the protein into solution conditions found in the commercially available FoldIt kit (Hampton Research) except that 7 M guanidine hydrochloride was included in the final dialysis buffer. Microdialysis buttons were then stepwise dialysed into water, gradually reducing the buffer concentration over a period of two weeks. Initial conditions for bulk protein precipitation were explored using the commercially available protein crystallization kits Crystal Screens 1 and 2, MembFac screen and Wizard crystallization kits (Hampton Research, Emerald Biostructures). Using the hanging-drop vapour-diffusion technique, 6 μl of purified protein (10 mg ml^{-1} for recombinant reflectin in 6 M guanidine hydrochloride) was mixed with 3 μl of well solution and allowed to actively diffuse against 1 ml (final volume) of well solution. A single condition was used for bulk precipitation of the recombinant reflectin protein and was accomplished by mixing 500 μl of purified protein with 300 μl of 15% methanol v/v, 0.1 M Zn(OAc) and 0.1 M morpholineethanesulphonic acid pH 6.0 (identified from Wizard II crystal screen) in a microcentrifuge tube and allowed to sit for ~10 h. The solution was then centrifuged at 20,000 × *g* for 1 min at 20 °C to pellet the recombinant protein.

FLOW COATING OF RECOMBINANT REFLECTIN FROM HFIP SOLUTIONS

Precipitated reflectin was redissolved in HFIP. 75 μl of the reflectin/HFIP solution was injected under the blade of the flow-coating apparatus set 50 μm above a silicon-wafer substrate. The silicon-wafer substrate was directionally translated at constant velocity (10 mm s^{-1}) for 50 mm, casting a uniform thin film. Gradient films were cast by adjusting the blade tilt by approximately 5°. Films were heated at 80 °C to remove residual HFIP from the film.

SPECTRAL MEASUREMENTS OF RECOMBINANT THIN FILMS

Spectral data of reflectin films were obtained using an Ocean Optics spectrometer with a functional range from 400 to 800 nm with a 1.5 nm resolution. Reflected light was collected using an Ocean Optics integrating sphere. A broadband halogen white-light source was used to illuminate the sample and spectra were collected at normal incidence.

CREATION OF SURFACE DIFFRACTION GRATINGS FROM IONIC LIQUID SOLUTIONS

Precipitated reflectin was redissolved in BMIM to a final concentration of 35% w/w. The solution was cast onto a silicon-wafer (glass slides can also be used) substrate using a Gardner draw-down bar to generate thin films. Submicrometre films were dipped into deionized water (or 0.5 to 1.0 M NaCl solution) at room temperature with varying speeds ranging from 5—50 mm s^{-1}. The silicon wafer and resultant grating were blown dry with nitrogen gas following their removal from the water bath.

WHITE-LIGHT INTERFEROMETRY

White-light interferometry was carried out on a VEECO NT1100 instrument using vertical scanning interferometry. Single scans were carried out for film-swelling measurements and 16 scans were averaged for diffraction gratings.

WIDE-ANGLE XRD

Wide-angle XRD experiments were carried out using a rotating-anode generator, a copper radiation source and a Stratton camera.

Received 31 January 2007; accepted 2 May 2007; published 3 June 2007.

References

1. Vukusic, P. & Sambles, J. R. Photonic structures in biology. *Nature* **424**, 852–855 (2003).
2. Onslow, H. On a periodic structure in many insect scales and the cause of their iridescent colours. *Phil. Trans. R. Soc. Lond. B* **211**, 1–74 (1921).
3. Berthier, S. *Iridescences: The Physical Colours of Insects* (Springer, Berlin, 2006).
4. Johnsen, S. Cryptic and conspicuous colouration in the pelagic environment. *Proc. R. Soc. Lond. B* **269**, 243–256 (2002).
5. Johnsen, S. & Sosik, H. M. Cryptic colouration and mirror sides as camouflage strategies in near-surface pelagic habitats: Implications for foraging and predator avoidance. *Limnol. Oceanogr.* **48**, 1277–1288 (2003).
6. Griffiths, D. J., Winsor, H. & Luong-Van, T. Iridophores in the mantle of giant clams. *Aust. Zool.* **40**, 319–326 (1992).
7. Crookes, W. J. *et al.* Reflectins: The unusual proteins of squid reflective tissues. *Science* **303**, 235–238 (2004).
8. Land, M. F. The physics and biology of animal reflectors. *Prog. Biophys. Mol. Biol.* **24**, 75–106 (1972).
9. Denton, E. J., Land, F. R. S. & Land, M. F. Mechanisms of reflexion in silvery layers of fish and cephalopods. *Proc. R. Soc. Lond. A* **178**, 43–61 (1971).
10. Denton, E. J. On the organization of reflecting surfaces in some marine animals. *Phil. Trans. R. Soc. B* **258**, 285–313 (1970).
11. McFall-Ngai, M. J. & Montgomery, M. K. The anatomy and morphology of the adult bacterial light organ of Euprymna scolopes Berry (Cephalopoda: Sepiolidae). *Biol. Bull.* **147**, 332–339 (1990).
12. Montgomery, M. K. & McFall-Ngai, M. J. The muscle-derived lens of a squid bioluminescent organ is biochemically convergent with the ocular lens. Evidence for recruitment of aldehyde dehydrogenase as a predominant structural protein. *J. Biol. Chem.* **267**, 20999–21003 (1992).
13. Weiss, J. L. *et al.* Methionine-rich repeat proteins: A family of membrane-associated proteins which contain unusual repeat regions. *Biochim. Biophys. Acta* **1668**, 164–174 (2005).
14. Cooper, K. M. & Hanlon, R. T. Correlation of iridescence with changes in iridophore platelet ultrastructure in the squid Lolliguncula brevis. *J. Exp. Biol.* **121**, 451–455 (1986).
15. Cooper, K. M., Hanlon, R. T. & Budelmann, B. U. Physiological colour change in squid iridophores II. Ultrastructural mechanisms in *Lolliguncula brevis*. *Cell Tissue Res.* **259**, 15–24 (1990).
16. Mäthger, L. M., Collins, T. F. T. & Lima, P. A. The role of muscarinic receptors and intracellular Ca^{2+} in the spectral reflectivity changes of squid iridophores. *J. Exp. Biol.* **207**, 1759–1769 (2004).
17. Fincham, A. G., Moradian-Oldak, J. & Simmer, J. P. The structural biology of developing dental enamel. *J. Struct. Biol.* **126**, 270–299 (1999).
18. Eastoe, J. E. Organic matrix of tooth enamel. *Nature* **187**, 411–412 (1960).
19. Du, C., Falini, G., Fermani, S., Abbot, C. & Moradian-Oldak, J. Supramolecular assembly of amelogenin nanospheres into birefringent microribbons. *Science* **307**, 1450–1454 (2005).
20. Makin, O. S. & Serpell, L. C. Structures for amyloid fibrils. *Fed. Eur. Bioch. Soc. J.* **272**, 5950–5961 (2005).
21. Swatloski, R. P., Spear, R. K., Holbrey, J. D. & Rogers, R. D. Dissolution of cellulose with ionic liquids. *J. Am. Chem. Soc.* **124**, 4974–4975 (2002).
22. Phillips, D. M. *et al.* Dissolution and regeneration of Bombyx mori silk fibroin using ionic liquids. *J. Am. Chem. Soc.* **126**, 14350–14351 (2004).
23. Sundd, M., Kundu, S. & Jagannadham, M. V. Alcohol-induced conformational transitions in ervatamin C. An alpha-helix to beta-sheet switchover. *J. Protein Chem.* **19**, 169–176 (2000).
24. Kumaran, S. & Roy, R. P. Helix-enhancing propersity of fluoro and alkyl alcohols: Influence of pH, temperature and cosolvent concentration on the helical conformation of peptides. *J. Pep. Res.* **53**, 284–293 (1999).
25. Ober, C. Persistence pays off. *Science* **296**, 859–861 (2002).
26. Qi, M. *et al.* A three-dimensional optic photonic crystal with designed point defects. *Nature* **429**, 538–542 (2004).

Acknowledgements

This work has been financially supported by DARPA (DSO) and AFOSR. We acknowledge M. McFall-Ngai (NIH AI50611) and E.G. Ruby (NIH RR 12294) for providing us with squid tissue. We thank M. Gupta for assistance with white-light interferometry imaging and D. Morse, R. Hanlon and M. Yustak for helpful discussions.
Correspondence and requests for materials should be addressed to R.R.N.
Supplementary Information accompanies this paper on www.nature.com/naturematerials.

Competing financial interests

The authors declare no competing financial interests.

Reprints and permission information is available online at http://npg.nature.com/reprintsandpermissions/

©2007 Nature Publishing Group